INTERNATIONAL JOURNAL OF OPTIMIZATION IN CIVIL ENGINEERING
Int. J. Optim. Civil Eng., 2024; 14(1):115-138

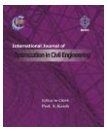

INTRODUCTION OF SHELL ELEMENT FOR FINITE ELEMENT ANALYSIS USING GRAPH-THEORETICAL FORCE METHOD

I. Karimi[1], M.S. Masoudi[2,*,†]
[1]*School of Civil Engineering, College of Engineering, University of Tehran, Tehran, Iran.*
[2]*Department of civil engineering, West Tehran branch, Islamic Azad University, Tehran, Iran.*

[DOI: 10.22068/ijoce.2024.14.1.578]

ABSTRACT

The main part of finite element analysis via the force method involves the formation of a suitable null basis for the equilibrium matrix. For an optimal analysis, the chosen null basis matrices should exhibit sparsity and banding, aligning with the characteristics of sparse, banded, and well-conditioned flexibility matrices. In this paper, an effective method is developed for the formation of null bases of finite element models (FEMs) consisting of shell elements. This leads to highly sparse and banded flexibility matrices. This is achieved by associating specific graphs to the FEM and choosing suitable subgraphs to generate the self-equilibrating systems (SESs) on these subgraphs. The effectiveness of the present method is showcased through two examples.

Kewords: Finite element force method, graph theory, shell element, null basis matrix, flexibility matrix.

Received: 30 October 2023; Accepted: 13 January 2024

1. INTRODUCTION

The force method of structural analysis, where the member forces are treated as unknowns, is appealing to researchers because the properties of the structure's members typically rely more on the member forces than on joint displacements. The force method was extensively utilized until 1960. The advent of digital computers and the applicability of the displacement method influenced most engineers to adopt the force method. In fact, the excellence of the force method in nonlinear analysis and optimization has been overlooked. In the force

[*]Corresponding author: Department of civil engineering, West Tehran branch, Islamic Azad University, Tehran, Iran.
[†]E-mail address: masoudi.ms@wtiau.ac.ir (M.S. Masoudi)

analysis approach, the quantity of equations to be resolved corresponds directly to the degree of statical indeterminacy (DSI) exhibited by the model. On the other hand, the displacement method entails a quantity of equations that is in parity with the degree of kinematical indeterminacy (DKI), commonly recognized as degrees of freedom (DOF). In scenarios where DSI is lesser than DOF, opting for the force method might prove beneficial. One notable advantage of the force method is its prompt accessibility to member forces, a pivotal necessity in the realm of reliability analysis.

Yet another benefit of the force method lies in its applicability to various redesign challenges and nonlinear elastic analyses. This method enables the resolution of modified problems without the need to recommence computations from the initial stages. In scenarios involving the optimal design of a structure with a predetermined topology, requiring numerous analyses, the force method can offer advantages. The statical basis remains consistent for each design across diverse loading cases, contributing to time savings in computations when contrasted with the displacement approach. Apart from these advantageous aspects, the theoretical appeal of extending the force method as a counterpart to the displacement method is significant. For an in-depth clarification of the duality concept, interested readers are recommended to consult the work of Argyris and Kelsey [1]. As will be demonstrated later, in employing this technique for structural analysis, MATLAB is employed to compute the flexibility matrix for each element. Subsequently, a block-diagonal flexibility matrix is formed from the element's matrix. However, in the displacement method, the global stiffness matrix of the structure is assembled from the individual stiffness matrices of elements. This step consumes a substantial amount of time in the structural analysis using the displacement method.

There are five distinct approaches that can be adopted in structural analysis using the force method, as follows: (i) topological force methods, (ii) graph theoretical methods, (iii) algebraic force methods, (iv) mixed algebraic-combinational force methods, (v) integrated force method.

Topological force methods for rigid-jointed skeletal structures have been developed by Henderson [2], Maunder [3] and Henderson and Maunder [4]. Methods suitable for computer methods are due to Kaveh [5]. Graph theoretical techniques based on cycle bases within the graph models were pioneered by Kaveh [6]. These methods are extended to encompass various categories of skeletal structures, including rigid-jointed frames, pin-jointed planar trusses, and ball-jointed space trusses in [7 and 8]. Algebraic techniques have been established by Denke [9], Robinson [10], Topçu [11], Kaneko *et al*. [12], and Soyer and Topçu [13]. Combined algebraic-topological approaches have been employed by Gilbert et al. [14], Coleman and Pothen [15 and 16], Pothen [17], and Heath *et al*. [18]. The integrated force method has been advanced by Patnaik [19 and 20], in which the equilibrium and compatibility conditions are simultaneously met using element force variables. Simultaneous analysis and design by force method can be found the work of Kaveh and Rahami [21].

In force method, the utilization of graph theoretical approaches is categorized into two classes of finite element models. The first category pertains to the forces along the edges of the elements [22-25], while the second category pertains to the forces concentrated at the mid-edge of the elements [26]. In this study, an effective approach is devised for generating a null basis for finite element models consisting of rectangular shell elements, resulting in

[DOI: 10.22068/ijoce.2024.14.1.578]

highly sparse and banded flexibility matrices. This method can be employed for optimal finite element analysis using the force method. This is accomplished by connecting a specific graph to the finite element model and opting for subgraphs (known to as γ-cycles [7]) to create localized self-equilibrating stress systems (null vectors). Their numerical values are computed through an algebraic procedure in MATLAB. As demonstrated in this study, the current approach exhibits efficiency and accuracy compared to alternative methods. The superiority of this technique will be illustrated using straightforward examples.

2. FORMULATION OF FORCE METHOD

Consider a discrete or discretized structure characterized by static indeterminacy. The m-dimensional vector $\boldsymbol{r}$ comprises independent forces acting on elements (members), and the n-dimensional vector $\boldsymbol{p}$ represents the nodal loads. The equilibrium equations of the structure can then be formulated as:

$$\boldsymbol{A}\boldsymbol{r} = \boldsymbol{p} \tag{1}$$

where $\boldsymbol{A}$ is an $n \times m$ equilibrium matrix, $\boldsymbol{r}$ is an m-dimensional vector containing the independent element forces, and $\boldsymbol{p}$ is an n-dimensional nodal load vector. Since the structure is assumed to be stable the equilibrium matrix will have full rank, i.e. $t = m - n > 0,\ rank(\boldsymbol{A}) = n$.

The member forces can be written as the sum of the particular and complementary solutions, where $\boldsymbol{q}$ is the t-dimensional vector of the redundant forces.

$$\boldsymbol{r} = \boldsymbol{B}_0\boldsymbol{p} + \boldsymbol{B}_1\boldsymbol{q} \tag{2}$$

$\boldsymbol{B}_0$ and $\boldsymbol{B}_1$ have m rows and n, and t columns, respectively. Pre-multiplying both sides of Equation (2) by $\boldsymbol{A}$ and utilizing Equation (1) results in:

$$\boldsymbol{A}\boldsymbol{B}_0 = \boldsymbol{I} \tag{3}$$

$$\boldsymbol{A}\boldsymbol{B}_1 = 0 \tag{4}$$

In these relations $\boldsymbol{B_0}$ and $\boldsymbol{B_1}$ are not unique for a structure, and numerous matrices of this kind can be generated. $\boldsymbol{B_1}$ is referred to as a static basis or self-stress matrix. This basis is termed a null basis in mathematics, and each column of the null basis matrix is identified as a null vector. The null space and null vectors serve as mathematical equivalents to the complementary solution space and self-equilibrating systems, respectively.

Minimizing the complementary potential energy subjected to the constraint as in Eq. (1) requires $\boldsymbol{r}$ to minimize the quadratic form

[DOI: 10.22068/ijoce.2024.14.1.578]

$$\mathbf{min}\boldsymbol{imize}(\frac{1}{2}\boldsymbol{r}^{t}\boldsymbol{F}_{m}\boldsymbol{r}) \tag{5}$$

Here, $\boldsymbol{F}_{m}$ is a $m \times m$ block diagonal matrix known as the unassembled flexibility matrix containing the flexibility matrices of the elements of a structure in its block diagonal entries. Combining Eq. (5) and Eq. (2) leads to

$$\boldsymbol{q} = -(\boldsymbol{B}_1^{t}\boldsymbol{F}_{m}\boldsymbol{B}_1)^{-1}(\boldsymbol{B}_1^{t}\boldsymbol{F}_{m}\boldsymbol{B}_0)\boldsymbol{p} \tag{6}$$

Solving this set of equations with accordance to Eq. (6), redundant forces can be obtained. After calculating the member forces, using the load-displacement relationship for each member, member distortions can be obtained as

$$[\boldsymbol{u}] = \left[\ \boldsymbol{F}_{m}\ \right][\boldsymbol{r}] = \left[\ \boldsymbol{F}_{m}\ \right]\left[\ \boldsymbol{B}_{0} \quad \boldsymbol{B}_{1}\ \right]\begin{bmatrix} \boldsymbol{p} \\ \boldsymbol{q} \end{bmatrix} \tag{7}$$

Nodal displacements can be calculated by virtual work as

$$[\nu_0] = [\boldsymbol{B}_0^{t}][\boldsymbol{u}] \tag{8}$$

Combining Eq. (7) and Eq. (8) leads to

$$\nu_0 = \boldsymbol{B}_0^{t}\boldsymbol{F}_{m}\boldsymbol{B}_0\boldsymbol{p} + \boldsymbol{B}_0^{t}\boldsymbol{F}_{m}\boldsymbol{B}_1\boldsymbol{q} \tag{9}$$

Substituting Eq. (6) in Eq. (9) leads to

$$\nu_0 = [\boldsymbol{D}_{00} - \boldsymbol{D}_{01}\boldsymbol{D}_{11}^{-1}\boldsymbol{D}_{10}]\boldsymbol{p} = \boldsymbol{F}\boldsymbol{p} \tag{10}$$

where $\boldsymbol{D}_{ij} = \boldsymbol{B}_i^{t}\boldsymbol{F}_{m}\boldsymbol{B}_j$. Therefore, the overall flexibility matrix of structure is obtained as

$$\boldsymbol{F} = \boldsymbol{D}_{00} - \boldsymbol{D}_{01}\boldsymbol{D}_{11}^{-1}\boldsymbol{D}_{10} \tag{11}$$

The effectiveness of an optimal analysis relies on the necessary computational time and storage for constructing the matrix and its attributes, such as sparsity and structuring (e.g., bandedness), along with its conditioning. To attain optimal analysis through the formation of an appropriate matrix $\boldsymbol{G}$, it is essential to choose a fitting $\boldsymbol{B_1}$ matrix.

Various algebraic methods, relying on different matrix factorizations like Gauss-Jordan elimination, LU, QR, and LQ, are available for creating a null basis matrix $\boldsymbol{B_1}$ from an equilibrium matrix $\boldsymbol{A}$ [14,18,28]. A concise overview of the fundamental principles behind these techniques is presented below. Suppose matrix A is partitioned using a column

[DOI: 10.22068/ijoce.2024.14.1.578]

permutation matrix $\boldsymbol{P}$ as follows:

$$\boldsymbol{AP} = [\boldsymbol{A}_1, \boldsymbol{A}_2] \tag{12}$$

where $\boldsymbol{A}_1$ is a $n \times n$ non-singular matrix. The matrix $\boldsymbol{B_1}$ can be written as

$$\left[\boldsymbol{B}_1\right] = \boldsymbol{P}\begin{bmatrix} -\boldsymbol{A}_1^{-1}\boldsymbol{A}_2 \\ \boldsymbol{I} \end{bmatrix} \tag{13}$$

2.1. LU decomposition method

By employing the LU decomposition method, the LU factorization of $\boldsymbol{A}$ is acquired as follows:

$$\boldsymbol{PA}=\boldsymbol{LU} \text{ and } \boldsymbol{U}\bar{\boldsymbol{P}} = [\boldsymbol{U}_1, \boldsymbol{U}_2] \tag{14}$$

$\boldsymbol{P}$ and $\bar{\boldsymbol{P}}$ are permutation matrices of order $n \times n$ and $m \times m$, respectively. Subsequently, $\boldsymbol{B_0}$ and $\boldsymbol{B}$ can be expressed as:

$$\left[\boldsymbol{B}_0\right] = \bar{\boldsymbol{P}}\begin{bmatrix} -\boldsymbol{U}_1^{-1}\boldsymbol{L}^{-1}\boldsymbol{p} \\ 0 \end{bmatrix} \text{ and } \left[\boldsymbol{B}_1\right] = \bar{\boldsymbol{P}}\begin{bmatrix} -\boldsymbol{U}_1^{-1}\boldsymbol{U}_2 \\ \boldsymbol{I} \end{bmatrix} \tag{15}$$

2.2. QR decomposition method

Using a QR factorization algorithm with column pivoting yields, where $\boldsymbol{P}$ is again a permutation matrix, and $\boldsymbol{R_1}$ is an upper triangular matrix of order n. $\boldsymbol{B_1}$ can be obtained as:

$$\boldsymbol{AP} = \boldsymbol{Q}[\boldsymbol{R}_1, \boldsymbol{R}_2] \tag{16}$$

$$\left[\boldsymbol{B}_1\right] = \boldsymbol{P}\begin{bmatrix} -\boldsymbol{R}_1^{-1}\boldsymbol{R}_2 \\ \boldsymbol{I} \end{bmatrix} \tag{17}$$

2.3. Turn-back method

Turn back method is available in [11,12] and is briefly outlined in this section. Expressing the matrix by column as $\boldsymbol{A}$= ($\boldsymbol{a_1}$, $\boldsymbol{a_2}$, $\boldsymbol{a_3}$,…,$\boldsymbol{a_n}$), a start column is designated as a column for which the ranks of ($\boldsymbol{a_1}$, $\boldsymbol{a_2}$, $\boldsymbol{a_3}$, …, $\boldsymbol{a_{s-1}}$) and ($\boldsymbol{a_1}$, $\boldsymbol{a_2}$, $\boldsymbol{a_3}$,…, $\boldsymbol{a_s}$) are identical. Put differently, $\boldsymbol{a}_s$ is a start column if it is linearly dependent on the lower-numbered columns. The coefficients of this linear dependency provide a null vector, and its highest-numbered non-zero component is in position $\boldsymbol{s}$. It is evident that the number of start columns is $t = m - n$, coinciding with the dimension of the null space of $\boldsymbol{A}$.

The start column can be determined by conducting a QR factorization on $\boldsymbol{A}$, employing orthogonal transformations to eliminate the sub-diagonal non-zeros. Assuming that, during the QR factorization, no column interchanges are made, and we simply bypass columns that

[DOI: 10.22068/ijoce.2024.14.1.578]

are already zero on and below the diagonal, the outcome will be a factorization in the subsequent format:

$$A = Q \begin{bmatrix} R \\ 0 \end{bmatrix} \tag{18}$$

The start columns are those columns where the upper triangular structure extends to the right. In other words, a column s is considered a start column if the highest non-zero position in column s of R is no greater than the highest non-zero position in earlier columns of R. The Turn-back method finds one null vector corresponding to each start column by 'turning back' from column s to identify the smallest k for which columns (a_s, a_{s-1}, a_{s-2},…, a_{s-k}) are linearly dependent. The null vector features non-zero elements exclusively in positions $s-k$ through s. Consequently, if k is relatively small for the majority of the start columns, the null basis will have a small profile. It is noteworthy that the Turn-back method operates on the A, and not on R. The initial QR factorization of A is solely used to ascertain the start columns and is subsequently discarded. The null vector identified by the Turn-back method from the start column a_s might not have non-zero elements in position s. Consequently, Turn-back requires some way to ensure that its null vectors are linearly independent. This assurance is achieved by preventing the left-most column involved in the dependency for each null vector from participating in any subsequent dependencies. Therefore, if the null vector associated with the start column a_s has its first non-zero element in position $s-k$, every null vector for a start column to the right of a_s will be zero in position $s-k$.

3. FLEXIBILITY MATRIX AND ELEMENT FORCES OF RECTANGULAR SHELL ELEMENT

A set of independent forces must be specified for creating the equilibrium matrix, A. In the finite element displacement method, nodal forces, S, are employed for structural analysis.[29] These forces are illustrated in Fig. 1. At each node, six nodal forces exist; thus, for an element with four nodes, $6\times N$ nodal forces can be identified.

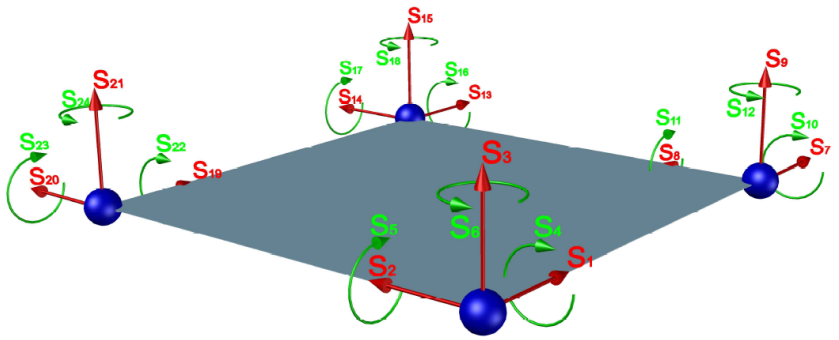

Figure 1. Nodal forces for shell element with four nodes

[DOI: 10.22068/ijoce.2024.14.1.578]

In the finite element force method, independent forces must be specified. Considering the six equilibrium equations, it follows that *6N-6* independent forces will be retained for an element with ***N*** nodes. These independent forces are referred to as element forces, ***F***, and are depicted in Fig. 2.

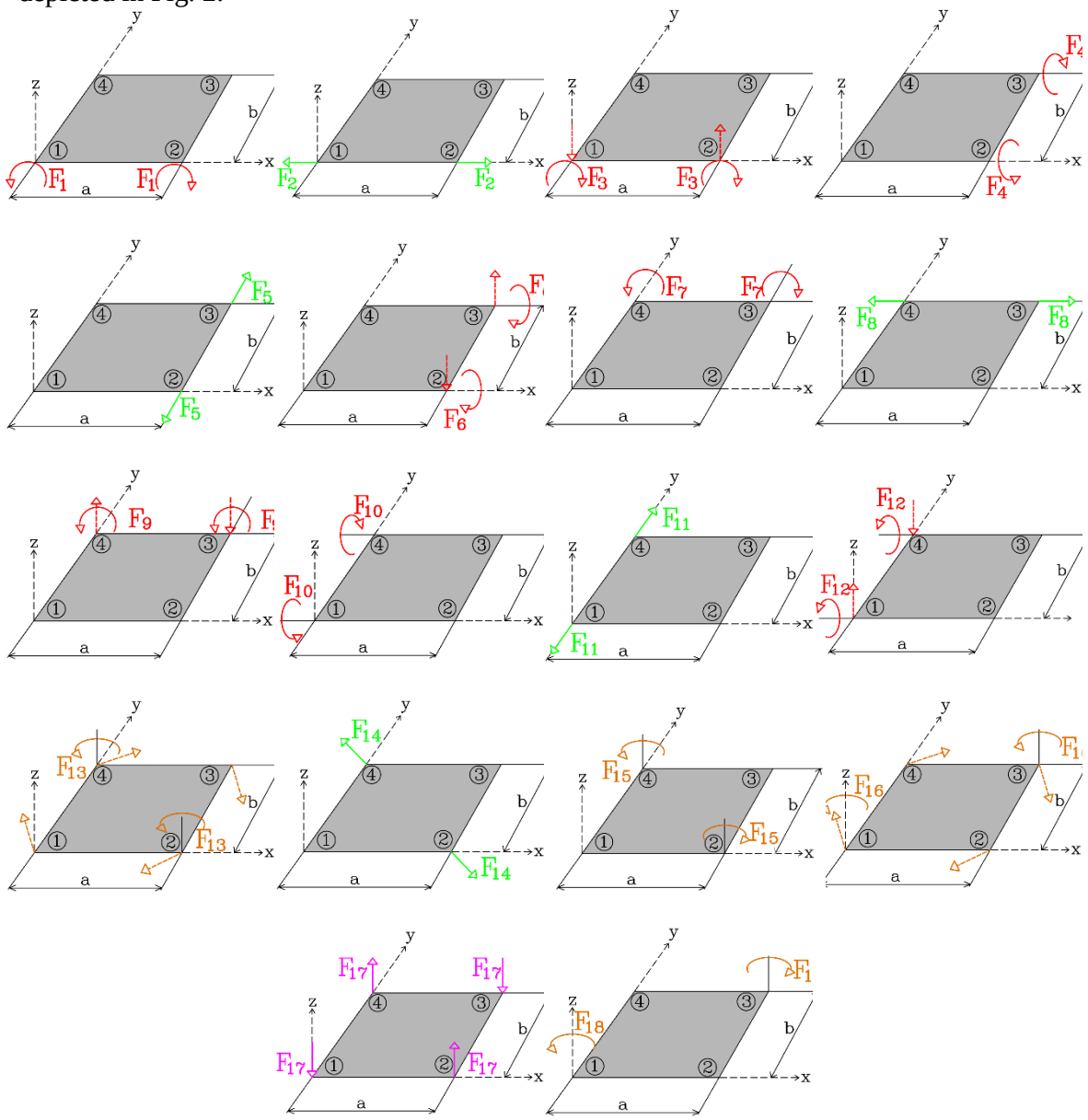

Figure 2. A set of independent forces for shell element with four nodes

These element forces are related to nodal forces through a transformation matrix, ***T***. In the case of an element with ***N*** nodes, this matrix comprises *6N* rows and *(6N-6)* columns. For a shell element with four nodes, this matrix can be characterized using Eq. (19) as:

[DOI: 10.22068/ijoce.2024.14.1.578]

$$\boldsymbol{S}=\boldsymbol{T}\times\boldsymbol{F}$$

$$T_{6N\times(6N-6)}=\begin{pmatrix}
0 & -1 & 0 & 0 & 0 & 0 & 0 & 0 & 0 & 0 & 0 & 0 & \frac{-b}{(a^2+b^2)} & 0 & 0 & \frac{-b}{(a^2+b^2)} & 0 & 0\\
0 & 0 & 0 & 0 & 0 & 0 & 0 & 0 & 0 & 0 & -1 & 0 & \frac{a}{(a^2+b^2)} & 0 & 0 & \frac{a}{(a^2+b^2)} & 0 & 0\\
0 & 0 & -\frac{2}{a} & 0 & 0 & 0 & 0 & 0 & 0 & 0 & 0 & \frac{2}{b} & 0 & 0 & 0 & 0 & -1 & 0\\
0 & 0 & 0 & 0 & 0 & 0 & 0 & 0 & 0 & 1 & 0 & 1 & 0 & 0 & 0 & 0 & 0 & 0\\
-1 & 0 & 1 & 0 & 0 & 0 & 0 & 0 & 0 & 0 & 0 & 0 & 0 & 0 & 0 & 0 & 0 & 0\\
0 & 0 & 0 & 0 & 0 & 0 & 0 & 0 & 0 & 0 & 0 & 0 & 0 & 0 & 0 & 1 & 0 & 1\\
0 & 1 & 0 & 0 & 0 & 0 & 0 & 0 & 0 & 0 & 0 & 0 & \frac{-b}{(a^2+b^2)} & \frac{a}{(a^2+b^2)^{0.5}} & 0 & \frac{-b}{(a^2+b^2)} & 0 & 0\\
0 & 0 & 0 & 0 & -1 & 0 & 0 & 0 & 0 & 0 & 0 & 0 & \frac{-a}{(a^2+b^2)} & \frac{-b}{(a^2+b^2)^{0.5}} & 0 & \frac{-a}{(a^2+b^2)} & 0 & 0\\
0 & 0 & \frac{2}{a} & 0 & 0 & -\frac{2}{b} & 0 & 0 & 0 & 0 & 0 & 0 & 0 & 0 & 0 & 0 & 1 & 0\\
0 & 0 & 0 & 1 & 0 & -1 & 0 & 0 & 0 & 0 & 0 & 0 & 0 & 0 & 0 & 0 & 0 & 0\\
1 & 0 & 1 & 0 & 0 & 0 & 0 & 0 & 0 & 0 & 0 & 0 & 0 & 0 & 0 & 0 & 0 & 0\\
0 & 0 & 0 & 0 & 0 & 0 & 0 & 0 & 0 & 0 & 0 & 0 & 1 & 0 & -1 & 0 & 0 & 0\\
0 & 0 & 0 & 0 & 0 & 0 & 0 & 1 & 0 & 0 & 0 & 0 & \frac{b}{(a^2+b^2)} & 0 & 0 & \frac{b}{(a^2+b^2)} & 0 & 0\\
0 & 0 & 0 & 0 & 1 & 0 & 0 & 0 & 0 & 0 & 0 & 0 & \frac{-a}{(a^2+b^2)} & 0 & 0 & \frac{-a}{(a^2+b^2)} & 0 & 0\\
0 & 0 & 0 & 0 & 0 & \frac{2}{b} & 0 & 0 & -\frac{2}{a} & 0 & 0 & 0 & 0 & 0 & 0 & 0 & -1 & 0\\
0 & 0 & 0 & -1 & 0 & -1 & 0 & 0 & 0 & 0 & 0 & 0 & 0 & 0 & 0 & 0 & 0 & 0\\
0 & 0 & 0 & 0 & 0 & 0 & 1 & 0 & -1 & 0 & 0 & 0 & 0 & 0 & 0 & 0 & 0 & 0\\
0 & 0 & 0 & 0 & 0 & 0 & 0 & 0 & 0 & 0 & 0 & 0 & 0 & 0 & 0 & 1 & 0 & -1\\
0 & 0 & 0 & 0 & 0 & 0 & 0 & -1 & 0 & 0 & 0 & 0 & \frac{b}{(a^2+b^2)} & \frac{-a}{(a^2+b^2)^{0.5}} & 0 & \frac{b}{(a^2+b^2)} & 0 & 0\\
0 & 0 & 0 & 0 & 0 & 0 & 0 & 0 & 0 & 0 & 1 & 0 & \frac{a}{(a^2+b^2)} & \frac{b}{(a^2+b^2)^{0.5}} & 0 & \frac{a}{(a^2+b^2)} & 0 & 0\\
0 & 0 & 0 & 0 & 0 & 0 & 0 & 0 & \frac{2}{a} & 0 & 0 & -\frac{2}{b} & 0 & 0 & 0 & 0 & 1 & 0\\
0 & 0 & 0 & 0 & 0 & 0 & 0 & 0 & 0 & -1 & 0 & 1 & 0 & 0 & 0 & 0 & 0 & 0\\
0 & 0 & 0 & 0 & 0 & 0 & -1 & 0 & -1 & 0 & 0 & 0 & 0 & 0 & 0 & 0 & 0 & 0\\
0 & 0 & 0 & 0 & 0 & 0 & 0 & 0 & 0 & 0 & 0 & 0 & 1 & 0 & 1 & 0 & 0 & 0
\end{pmatrix} \tag{19}$$

Formulation of a discrete element equivalent to the actual continuous structure is the first step in matrix structural analysis. For a linear system, the stresses are related to the forces F by following equation as:

$$\sigma=\bar{\boldsymbol{c}}\boldsymbol{F} \tag{20}$$

$\bar{c}$ is a matrix that shows a statically equivalent stress system due to the unit force $\boldsymbol{F}$. Now, the flexibility matrix can be calculated as follows with taking integration over the volume of the element

$$\boldsymbol{f_m}=\int_v \bar{\boldsymbol{c}}^t\varphi\bar{\boldsymbol{c}}\boldsymbol{dV} \tag{21}$$

In the above equation, φ is the matrix relating the stresses to strains in three dimensional problems as:

$$\varepsilon=\varphi\sigma \tag{22}$$

The creation of the flexibility matrix involves establishing the matrix $\bar{c}$. The ith column of $\bar{c}$ illustrates the resulting stresses due to a unit element force $\boldsymbol{F_i}$ in the force method.

[DOI: 10.22068/ijoce.2024.14.1.578]

Additionally, the resulting stresses caused by nodal forces $\boldsymbol{S}$ are identical to the ith column of $\boldsymbol{T}$ in the displacement method. By taking into account the preceding equations, matrix can be constructed for the shell element. Subsequently, the flexibility matrix of the element can be computed using the Gauss numerical integration method.

4. GRAPHS THEORY DEFINITIONS AND ITS APPLICATIONS IN FINITE ELEMENT FORCE METHOD

4.1. Basic graph theory definitions

A graph $\boldsymbol{S}$ consists of nodes $\boldsymbol{N(S)}$ and members $\boldsymbol{M(S)}$. When two distinct nodes are connected by a member, they are called adjacent. These nodes are the end nodes of a member, and a member is named incident with a node if it is an end node of the member. The number of members incident with a node is referred to as the degree of that node. A sub-graph $\boldsymbol{S_i}$ of a graph $\boldsymbol{S}$ is defined as a graph in which $\boldsymbol{N(S_i)\subseteq N(S)}$ and $\boldsymbol{M(S_i)\subseteq M(S)}$. Additionally, each member in $\boldsymbol{S_i}$ has the same endpoints as its corresponding member in $\boldsymbol{S}$.

A path of $\boldsymbol{S}$ is a finite sequence $\boldsymbol{P_i=\{n_0,m_1,n_1,...,m_p,n_p\}}$ where the terms are alternating and consist of distinct nodes $\boldsymbol{n_i}$ and distinct members $\boldsymbol{m_i}$ of S for $\boldsymbol{1 \le i \le p}$, and $\boldsymbol{n_{i-1}}$ and $\boldsymbol{n_i}$ are the two ends of $\boldsymbol{m_i}$. If there is a path between two nodes $\boldsymbol{n_i}$ and $\boldsymbol{n_j}$, they are considered connected in $\boldsymbol{S}$. A cycle is a path $\boldsymbol{(n_0,m_1,n_1,...,m_p,n_p)}$ for which $\boldsymbol{n_0 = n_p}$ and $\boldsymbol{p \ge 3}$; i.e. a cycle is a closed path. The cycles within a graph collectively constitute a vector space recognized as the cycle space. The size of this space for a connected graph $\boldsymbol{S}$ is termed *first Betti number*, denoted as $\boldsymbol{b_1(S)=M(S)-N(S)+1}$, where $\boldsymbol{M(S)}$ and $\boldsymbol{N(S)}$ represent the number of members and nodes in $\boldsymbol{S}$, respectively. To convey the topological characteristic of a finite element model into the connectivity of a graph, ten distinct graphs have been presented in [27,28]. Subsequently, an Interface Graph and an Associate Graph are introduced for a finite element model consisting of shell elements.

4.2. An Interface Graph

The construction of this graph for shell Finite Element Method (FEM) involves the following steps:

Step 1: All nodes within the Finite Element Model (FEM) are included in the Interface Graph (IG) of the FEM.

Step 2: For each edge of a shell element within the FEM, three graph members are taken into consideration.

Step 3: Three graph members are linked to each diagonal of an element within the FEM.

The depiction of this graph for an element can be seen in Fig. 3. The numbering of nodes and edges in the interface graph should align with the numbering system used in the Finite Element Model (FEM). For k^{th} element, the edges of the Interface Graph (IG) are assigned numbers as follows:

$$18(\boldsymbol{k}-1)+\boldsymbol{i};\boldsymbol{i}=1:18 \tag{23}$$

[DOI: 10.22068/ijoce.2024.14.1.578]

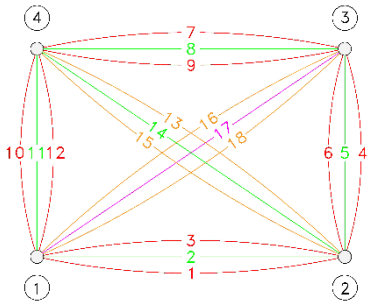

Figure 3. Interface graph for a shell element

The member numbering of the interface graph should be executed in accordance with the numbering of the FEM, considering the primary nodal numbering of a given element in the model. Consequently, for each rectangular element, 18 members of the interface graph will be numbered sequentially, following the patterns depicted in Fig. 4 for two, three, and four adjacent elements.

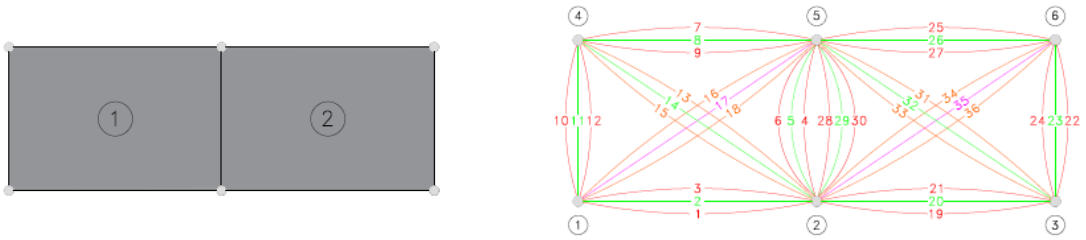

(a)

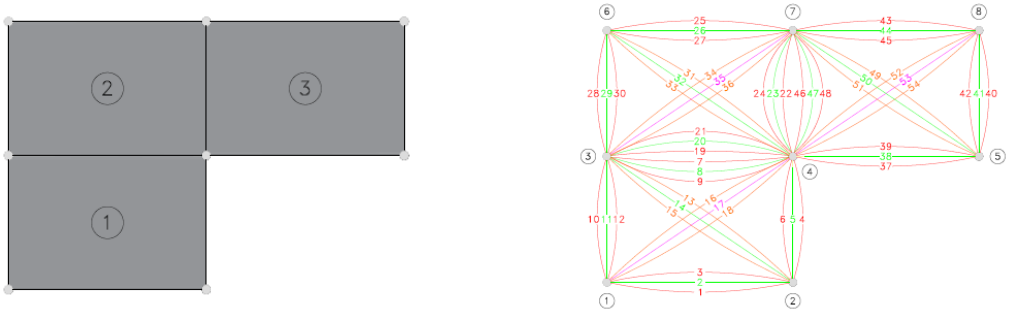

(b)

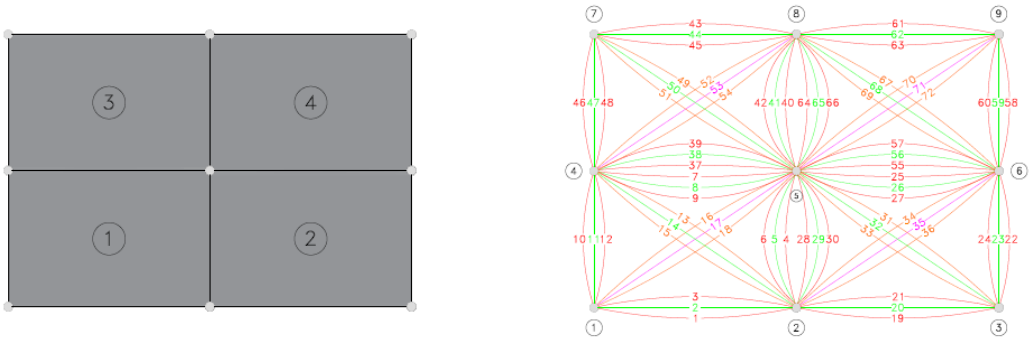

(c)

Figure 4. Interface graph for: (a) two elements, (b) three elements and (c) four elements

[DOI: 10.22068/ijoce.2024.14.1.578]

4.3. Natural associate graph

In this graph, each shell element of the FEM is associated with one node, and two nodes are connected by a member if the elements share a common edge. The creation of the NAG (Node-Adjacent Graph) for Finite Element Model (FEM) can be accomplished through the following procedure: A crucial initial phase in FEM involves defining the elements along with their interconnected nodes. This process results in the construction of the element connectivity matrix, encompassing the relationships between elements and nodes. Simultaneously, during the formulation of the element connectivity matrix, an additional matrix is generated, known as the node connectivity matrix, which encapsulates node-element incidence properties. By utilizing both the element connectivity and node connectivity matrices, an algorithm can be established, facilitating the efficient generation of NAG with a computational complexity of *O(n)*.

To identify the adjacent elements to the nth element that share either two common nodes or one common edge, the first step involves determining the connected nodes to the nth element from the element connectivity matrix. Subsequently, utilizing the node connectivity matrix, elements that have at least one common node with the nth element are identified. This reduced search space is then convenient for identifying the adjacent elements. Fig. 5 illustrates two Finite Element Models (FEMs) alongside their respective Natural associate graphs (NAGs).

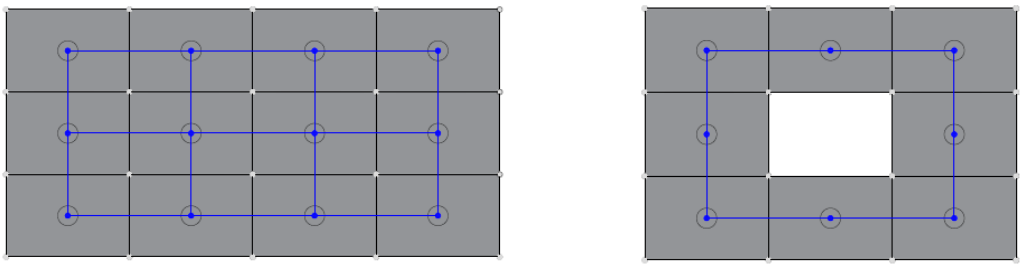

(a) (b)

Figure 5. NAG for two finite element models, (a) model with 12 elements and (b) model with an opening

5. PATTERN CORRESPONDING TO SELF-EQUILIBRATING SYSTEMS

5.1. Degree of static indeterminacy of the FEM

By considering the interface graph, each shell elements have 18 elemental forces, and Each nodes have 6 equilibrium equations. Thus, calculating the degree of static indeterminacy (DSI) and forming the self-equilibrating systems of the FEM are replaced by the DSI and self-equilibrating systems of the equivalent 3D skeletal model. In this way using the DSI of a space skeletal structure with N nodes and M members as, $DSI = M - 6N + 6$ the degree of indeterminacy of a FEM is obtained as

$$\boldsymbol{DSI = 18E - 6N + 6} \tag{24}$$

[DOI: 10.22068/ijoce.2024.14.1.578]

where *E* is the number of shell elements and *N* is the total number of the nodes of the FEM. With the above simulation, the patterns of the self-equilibrating systems can be identified as follows:

5.2. Pattern of type I self-equilibrating systems

Every set consisting of six members of the interface graph, corresponding to two elements of the FEM with common edges, is called a self-equilibrating system of Type I. The corresponding subgraph contains three SESs. Therefore, the set of six members corresponding to the common edges of the three elements ***i*** and ***j*** (***i*** < ***j***), has three members m_i, n_i and p_i (***m*<*n*<*p***), and r_j, s_j and t_j (***r*<*s*<*t***). The three SESs obtained from this set are as follows:

(m,r) with (-1,+1) and (n,s) with (-1,+1) and (p,t) with (+1,+1)

i.e. a null vector with non-zero entries (-1,1) in rows (m,r), another null vector with non-zero entries (-1,1) at ***(n,s)*** and another one with non-zero entries (+1,+1) at ***(p,t)*** are formed. The member with a bigger number is selected as the generator of the current SES and also as a redundant force. In other words, when two elements are positioned adjacently in the horizontal direction, members 4, 5, and 6 of the left element, along with members 10, 11, and 12 of the right element, collectively form three null vectors of type I and generators consist of selected members with higher numbers. Furthermore, in the case of two vertically adjacent elements, members 7, 8, and 9 of the lower element, alongside members 1, 2, and 3 of the upper element, collectively form three null vectors of type I. Additionally, generators with higher number are selectively chosen. Obviously, the number of such minimal SESs is triple the number of the members of the associate graph, since each member of this graph passes from the interface of two elements. Nearly, more than two-third of null vectors for a FEM are of this type, corresponding to high sparsity for the null basis matrix. For two adjacent elements, these non-zero entries of null basis matrix are shown in Fig. 6.

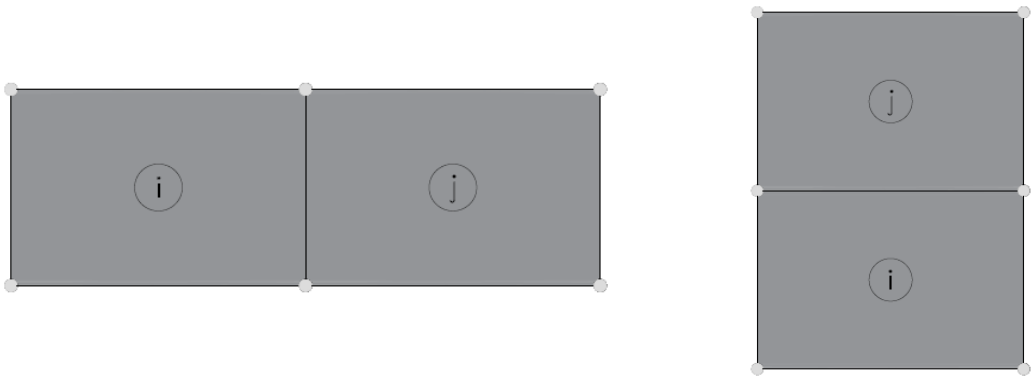

(a)

[DOI: 10.22068/ijoce.2024.14.1.578]

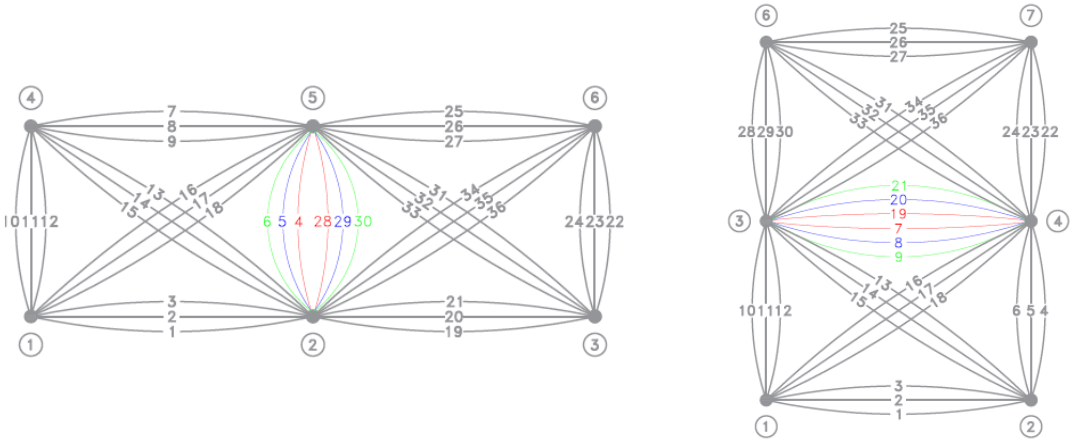

(b)

$$B_1^T = \begin{bmatrix} \dots & 4 & 5 & 6 & \dots & 28 & 29 & 30 & \\ & & & & & & & & \\ \dots & -1 & 0 & 0 & \dots & +1 & 0 & 0 & \dots \\ \dots & 0 & -1 & 0 & \dots & 0 & +1 & 0 & \dots \\ \dots & 0 & 0 & +1 & \dots & 0 & 0 & +1 & \dots \end{bmatrix} \qquad B_1^T = \begin{bmatrix} \dots & 7 & 8 & 9 & \dots & 19 & 20 & 21 & \dots \\ & & & & & & & & \\ \dots & -1 & 0 & 0 & \dots & +1 & 0 & 0 & \dots \\ \dots & 0 & -1 & 0 & \dots & 0 & +1 & 0 & \dots \\ \dots & 0 & 0 & +1 & \dots & 0 & 0 & +1 & \dots \end{bmatrix}$$

(c)

Figure 6. Two adjacent element and its type I SESs.

5.3. Pattern of type II self-equilibrating systems

For each two adjacent finite elements (two adjacent nodes in the associate graph) such as ***i*** and ***j*** (***i<j***), another type of SES can be constructed, which is called a self-equilibrating system of Type II. Two adjacent shell elements and their corresponding interface graphs are shown in Figure 7(a). The DSI of interface graph can be calculated as:

$$DSI = 18 \times 2 - 6 \times 6 + 6 = 6 \tag{25}$$

Thus, corresponding to three null vectors, Three null vectors are previously formed using six edges in the interface of two elements. Therefore, in order to form the other SESs, the generators of three type I SESs should be removed from interface subgraph.

$$TypeII = DSI - TypeI = 6 - 3 = 3 \tag{26}$$

It should be noted that each subgraph with DSI = 1 corresponds to a SES, the edge with the highest number is taken as the generator of that SES. Thus the DSI of remaining subgraph equals three and three independent null vectors can be easily extracted. Three generators should be selected from subgraphs for three null vectors of Type II. These members have been specified by red color in Figure 7(b). An algebraic method such as LU

[DOI: 10.22068/ijoce.2024.14.1.578]

or QR factorization can be used to calculate the numerical values of these three null vectors.

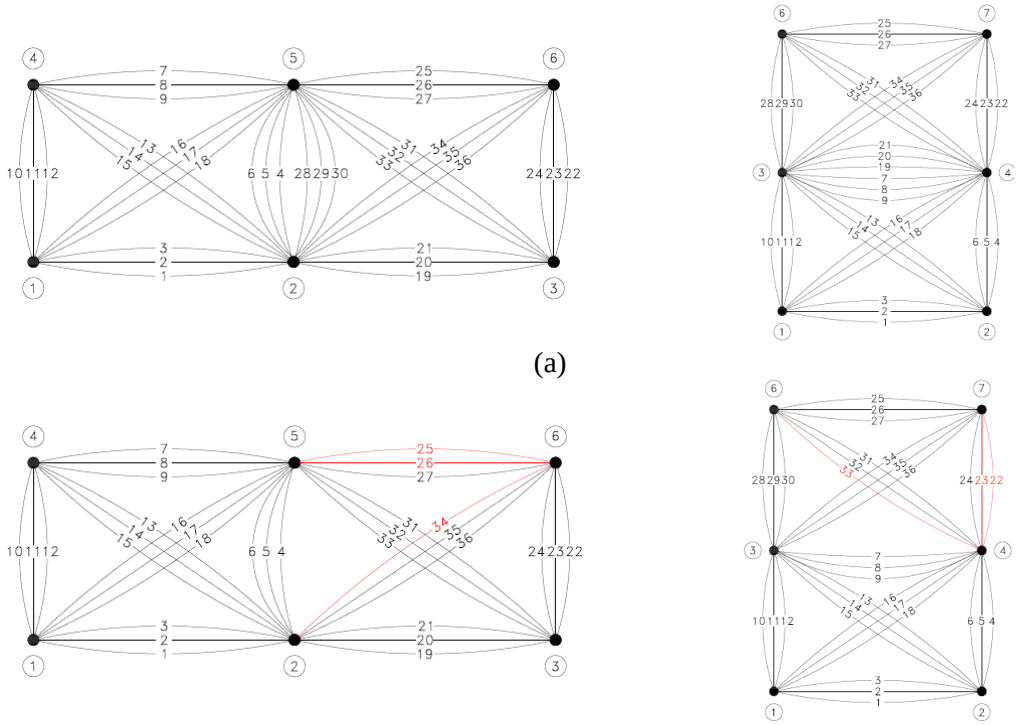

(a)

(b)

Figure 7. Two adjacent element and its type II SESs.

5.4. Pattern of type III self-equilibrating systems

In the previous sections, two types of SESs were defined. These systems are sufficient for forming null bases of finite element models without openings. However, if a FEM contains one or more openings, another type of SESs can be identified, known as self-equilibrating system of Type III. In fact, from each opening in the FEM, three independent SESs can be extracted. The subgraphs corresponding to these SESs usually have more edges than the previous systems, and also their related null vectors have more non-zero entries.

An opening can be found in model using cycle bases of associate graph. Every cycle of NAG(FEM) with more than 8 edges corresponds to an opening, as shown in Fig. 8.

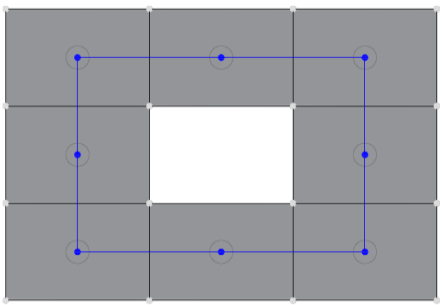

Figure 8. Natural associate graph

[DOI: 10.22068/ijoce.2024.14.1.578]

Every opening with *M* element has *18M* members in interface graph. The corresponding cycle has *M* member in associate graph. Thus *3M* SESs of type I and *3M* SESs of type II can be extracted from these *M* elements. For example, the DSI of model which is illustrated in Figure 8 is:

$$DSI = 18M - 6N + 6 = 18 \times 8 - 6 \times 16 + 6 = 54 \tag{27}$$

The number of type I & II is:

$$TypeI = 3 \times M = 3 \times 8 = 24 \tag{28}$$

$$TypeII = 3 \times M = 3 \times 8 = 24 \tag{29}$$

The remaining subgraph after deleting the generators of type I and II has DSI equal to 6 as:

$$TypeIII = \underbrace{54}_{DSI} - \underbrace{24}_{TypeI} - \underbrace{24}_{TypeII} = 6 \tag{30}$$

It means that six SESs can be extracted from remaining subgraph which are called SESs of Type III. i.e, for each opening, six SESs can be found which are not in previous SESs and are independent. An algebraic method can be used for calculating numerical values of these six null vectors.

6. GENERAL ALGORITHM

This algorithm consists of the following steps for generating null basis matrix for FEM comprising of shell elements:

Step 1: First, the model is elementalized using shell elements. Then, the nodes and elements are numbered appropriately and logically. To obtain a flexibility matrix with a suitable structure, existing algorithms can be employed for node and element numbering.

Step 2: NAG and Interface graphs are constructed based on the information provided in section 4 of this article. Members and nodes of these graphs are also labeled according to the numbering of the elements.

Step 3: Then the rectangular equilibrium matrix of the model is generated. The concepts of Kaveh and koohestani's article has been used to consider the support conditions in the equilibrium matrix.[30]

Step 4: Null vectors of type I are created for the adjacent elements as outlined in section 5, and the respective generators are also identified.

Step 5: Then, Null vectors of type II are generated for the adjacent elements as explained in section 5, and the corresponding generators are also recognized

Step 6: For each opening in the model, six null vectors are established, recognized as the

[DOI: 10.22068/ijoce.2024.14.1.578]

self-equilibrating system Type III.

Step 7: All null vectors of type I, II and III are placed together in matrix $\boldsymbol{B_1}$, forming the matrix of null vectors for the entire model. In this phase, if there is indeterminacy in the supports, the corresponding null vectors are also generated and added.

Step 8: Null vectors are sorted in ascending order according to the highest number of their non-zero components in the $\boldsymbol{B_1}$ matrix, resulting in the matrix of null bases being available for all models under support conditions.

7. NUMERICAL EXAMPLES

In this section two examples are studied. Models are assumed to be supported in a statically determinate or indeterminate fashion. The effect of indeterminate support conditions can separately be included with no difficulty [30-32]. However, the null basis matrices for each model are calculated using the present algorithm, LU factorization and QR factorization methods and the results are compared through computational time (scaled), sparsity, pattern of matrices and accuracy. Furthermore, the patterns of the flexibility matrix are evaluated by employing the three methods mentioned and compared in terms of structure and sparsity. In all the following examples, *nnz* represents the number of non-zero entries and λmax/λmin is the ratio of the extreme eigenvalues taken as the condition number of a matrix.

7.1. Example 1

Example 1 illustrates a wall structure that is statically indeterminate, as shown in Fig. 9. The finite element model shown in Fig. 9(a), comprising 190 shell elements and 266 nodes. The model is idealized using shell elements. The model has the following mechanical properties: Thickness = 0.3 m, E = 2.5e+9 kg/m^2, ν = 0.25.

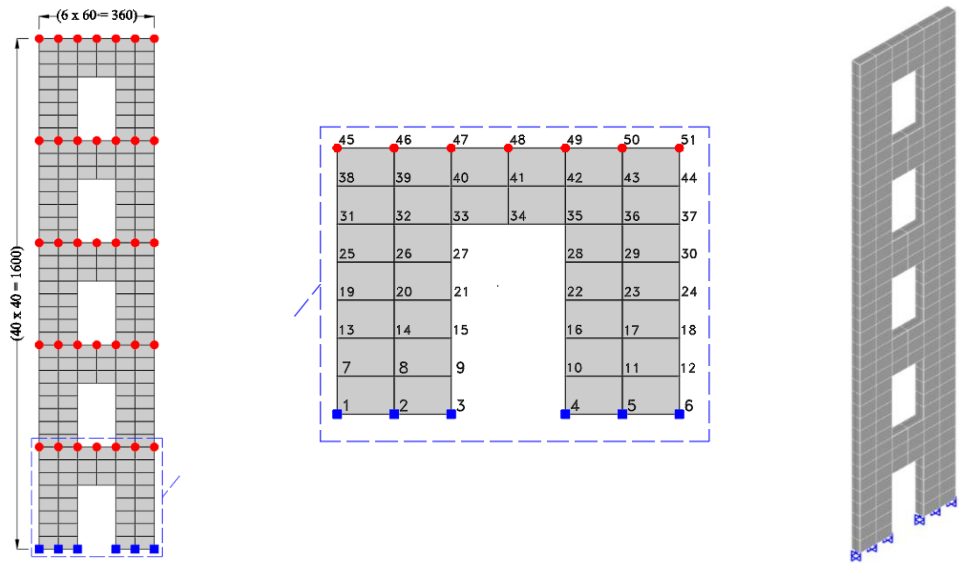

(a) (b) (c)

Figure 9. (a) Finite element model of Example 1, (b) node numbering of model, and (c) 3D view.

[DOI: 10.22068/ijoce.2024.14.1.578]

The interface graph and Natural associate graph of the model are shown in Fig. 10. The pattern of the equilibrium matrix is shown in Fig. 11. Fig. 12 depicts the pattern of the null basis matrices using the present method, LU factorization method and QR factorization method. The flexibility matrices are illustrated in Fig. 13. The displacement and rotation of blue nodes numbered 1 to 6 are constrained in all directions and are considered as fixed supports. Model loading specifications (kgf) in red points of the model are 50, 5, and -100 for X, Y, and Z directions, respectively.

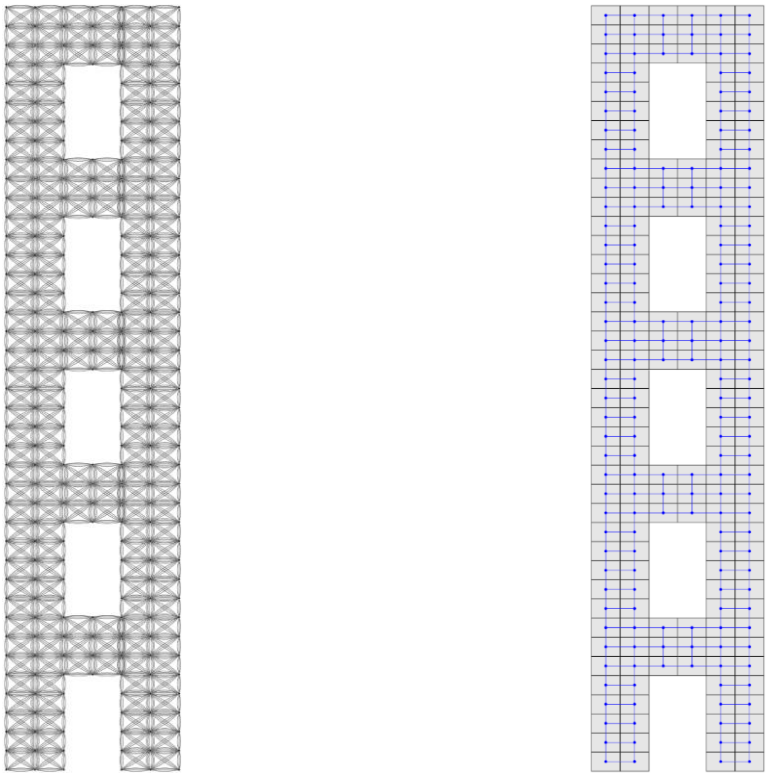

(a) (b)

Figure 10. (a) Interface graph of Example 1, (b Natural associate graph

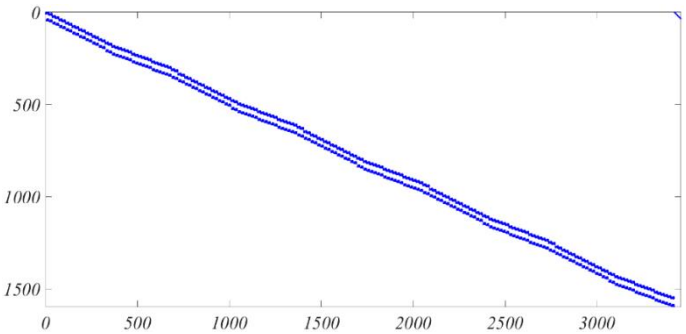

nz=12196

Figure 11. Pattern of the equilibrium matrix for Example 1.

[DOI: 10.22068/ijoce.2024.14.1.578]

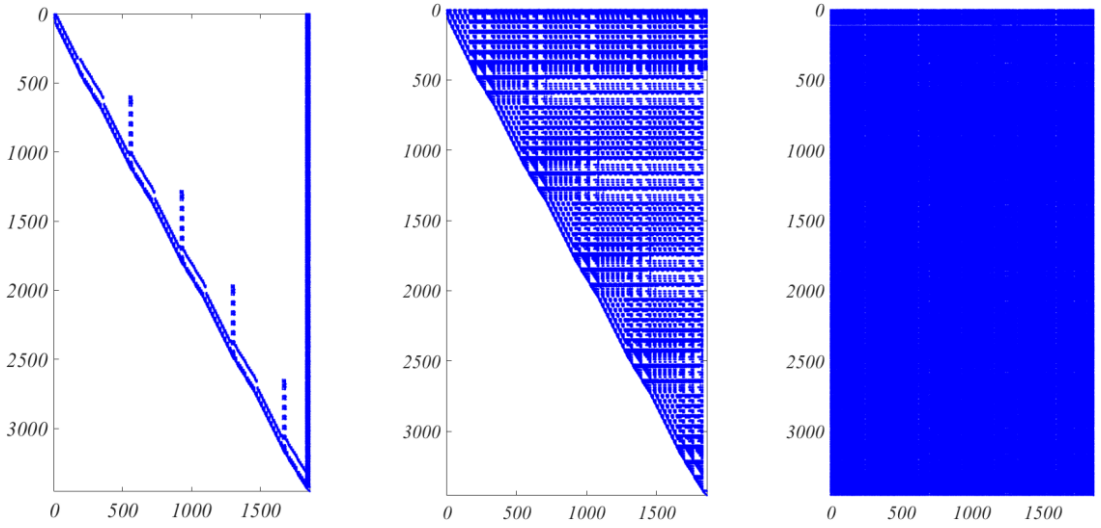

nz=26420 *nz=124544* *nz=756153*

(a) (b) (c)

Figure 12. Patterns and the number of non-zero entries of the null bases of Example 1: (a) Present algorithm, (b) LU factorization and (c) QR factorization.

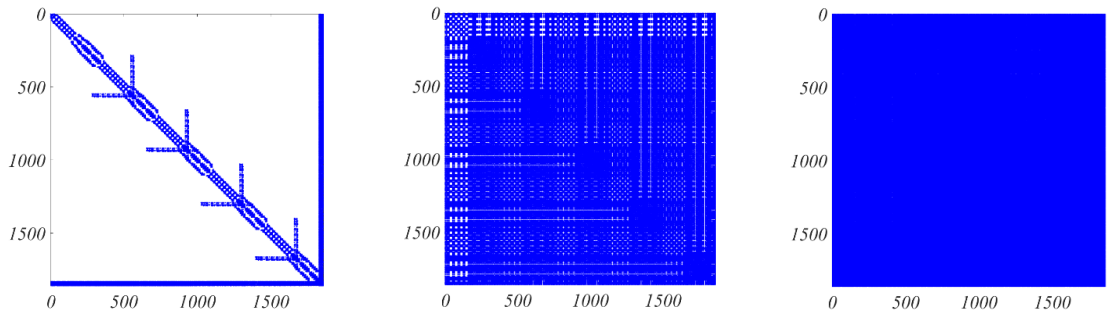

nz=48540 *nz=546524* *nz=1274982*

(a) (b) (c)

Figure 13. Patterns of the flexibility matrix $G = B_1^t F_m B_1$ for Example 1: (a) Present algorithm, (b) LU factorization and (c) QR factorization.

Table 1. Comparison of the optimality characteristics of the null basis matrices B1 and flexibility matrices G for the FEMs of Example 1

DSI	The number of each type of SESs			$\frac{nnz B_{1\ presentMethod}}{nnz B_{1\ LU\ method}}$	$\frac{nnz B_{1\ presentMethod}}{nnz B_{1\ QR method}}$	Condition Num. $\frac{\lambda_{max}}{\lambda_{min}}$ *for* $B_1^t B_1$			Norms max $\lvert A \times B_1 \rvert$		
	Type I	Type II	Type III			present	LU	QR	present	LU	QR
1830	903	903	24	0.2121	0.0349	4.8821e+5	6.3207e+6	6.3e2	3.5601e-14	2.3670e-13	2.0636e-10

[DOI: 10.22068/ijoce.2024.14.1.578]

7.2. Example 2

Example 2 illustrates a bridge structure that is statically indeterminate, as shown in Fig. 14. The finite element model shown in Fig. 14, comprising 324 shell elements and 370 nodes. The model is idealized using shell elements. All models share the same nodes and have the following mechanical properties: Thickness = 0.4 m, E = 2.5e+9 kg/m^2, ν = 0.25. The interface graph and Natural associate graph of the model are shown in Fig. 15. The pattern of the equilibrium matrix is shown in Fig. 16. Fig. 17 depicts the pattern of the null basis matrices using the present method, LU factorization method and QR factorization method. The flexibility matrices are illustrated in Fig. 18. The displacement of blue nodes are constrained in all directions and are considered as pinned supports. Model loading specifications (kgf) in red points in the middle of the model are 0, 0, and -100, in X, Y, and Z directions, respectively.

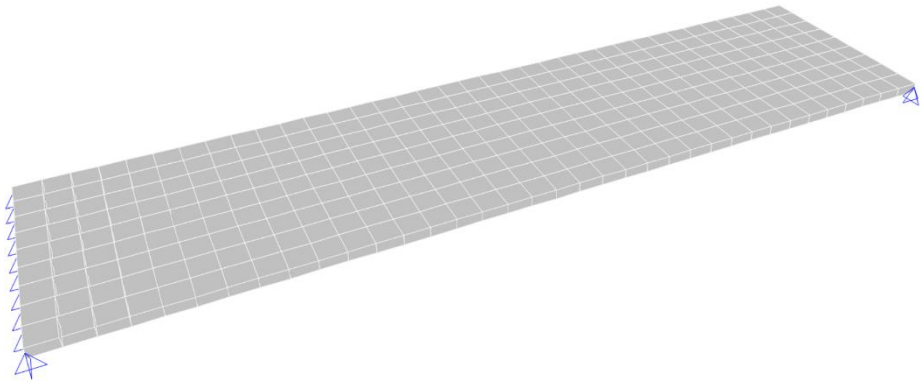

(a)

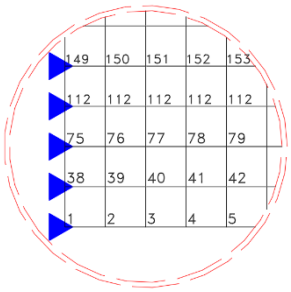

(b)

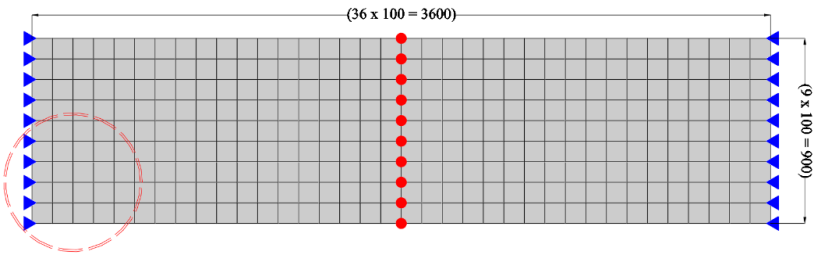

(c)

Figure 14. (a) 3D view of example 2, (b) Finite element model, (c) Node numbering of model

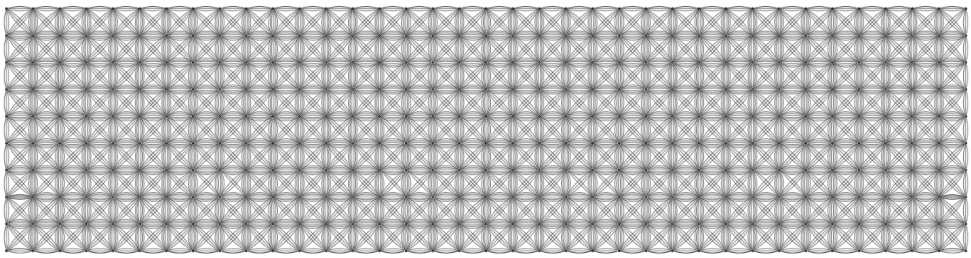

(a)

[DOI: 10.22068/ijoce.2024.14.1.578]

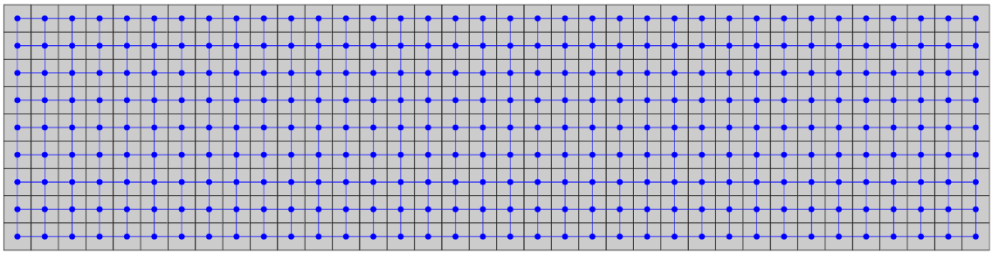

(b)

Figure 15. (a) Interface graph of Example 2, (b Natural associate graph

Tables 1 and 2, contains other optimality characteristics of the force method procedures. It is clear that the graph theoretical method forms the most well structured null basis in smallest computational time. The results of example 2 are verified by standard displacement method in Table 3.

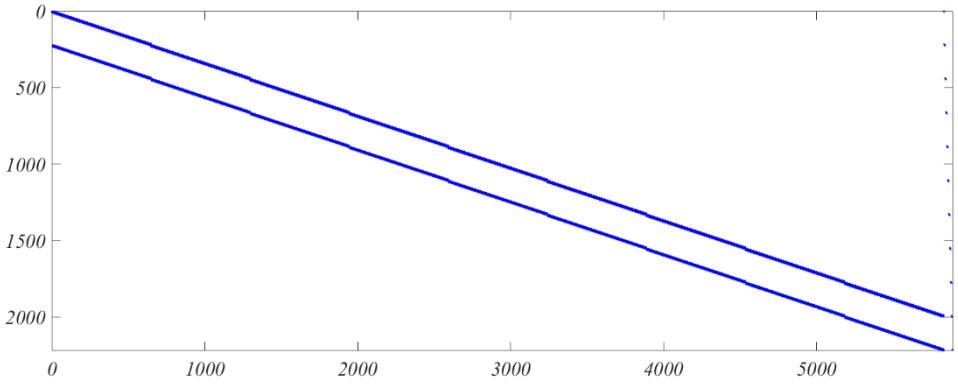

Figure 16. Pattern of the equilibrium matrix for Example 2.

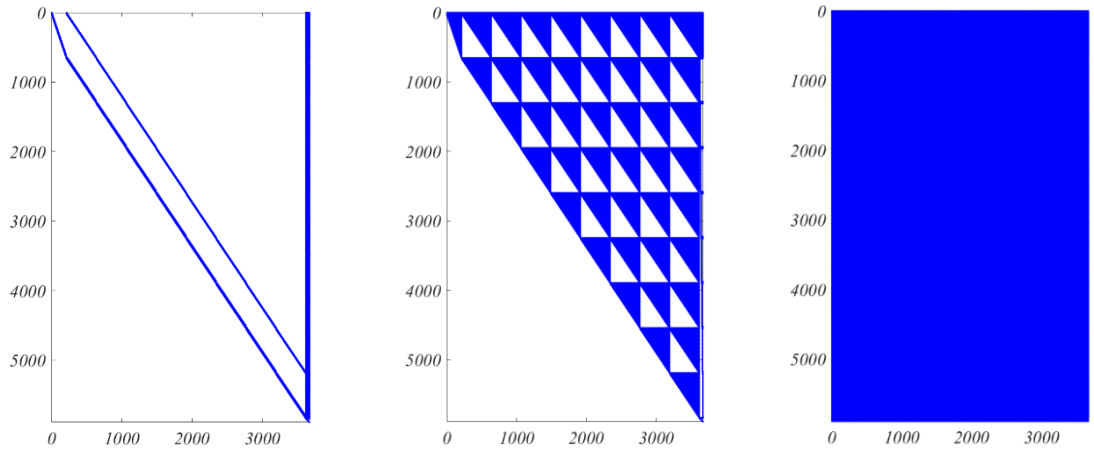

(a) (b) (c)

Figure. 17. Patterns and the number of non-zero entries of the null bases of Example 2: (a) Present algorithm, (b) LU factorization and (c) QR factorization.

[DOI: 10.22068/ijoce.2024.14.1.578]

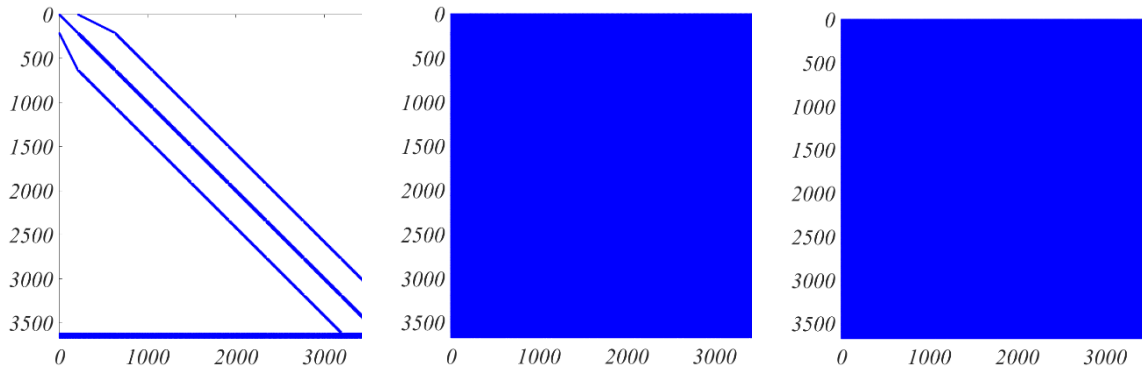

Figure 18. Patterns of the flexibility matrix $G = B_1^t F_m B_1$ for Example 2: (a) Present algorithm, (b) LU factorization and (c) QR factorization.

Table 2. Comparison of the optimality characteristics of the null basis matrices B1 and flexibility matrices G for the FEMs of Example 2

DSI	The number of each type of SESs			$\frac{nnzB_{1\ presentMethod}}{nnzB_{1\ LU\ method}}$	$\frac{nnzB_{1\ presentMethod}}{nnzB_{1\ QRmethod}}$	Condition Num. $\frac{\lambda_{max}}{\lambda_{min}}$ for $B_1^t B_1$			Norms max $\lvert A \times B_1 \rvert$		
	Type I	Type II	Type III			present	LU	QR	present	LU	QR
3618	1809	1809	0	0.2501	0.0234	1.8994e+03	1.0517e+07	6.8158e+03	2.2204e-16	7.3896e-13	2.0317e-14

Table 3. Comparison among deflections of 10 middle nodes of the bridge for Example 2 resulting by the displacement method and the present force method.

Number of middle (red) nodes	Z-deflection (mm)	
	Displacement method	Force method
19	-1.02266	-1.01884
56	-1.0131	-1.02105
93	-1.00613	-1.00123
130	-1.00158	-0.99512
167	-0.99932	-1.00687
204	-0.99932	-0.99252
241	-1.00158	-1.00321
278	-1.00613	-1.00115
315	-1.0131	-1.01650
352	-1.02266	-1.02490

[DOI: 10.22068/ijoce.2024.14.1.578]

7. CONCLUSIONS

The main conclusions of this paper are as follows:

The solution of many examples reveals that the present algorithm can achieve high accuracy.

The flexibility matrices obtained are highly sparse and narrowly banded. This is attributed to the utilization of regional cycles of the natural associate graphs and the appropriate ordering of the selected self-equilibrating systems.

The conditioning of the flexibility matrices generated by the present algorithm is superior to those formed by the LU method.

Because of a high reduction in the number of floating point operations, the resulted null basis has better accuracy in comparison to other methods, this is obvious since nearly 50% of the null vectors are selected without numerical analysis, and the remaining null vectors are obtained by working on small and limited lists.

The method developed in this paper can be easily extended to finite element models (FEMs) with higher-order elements. It should be noted that in the present method, the most crucial aspect is the selection of an independent element forces system.

The use of higher-order elements in the force method results in fewer unknowns compared to the displacement method.

The computational time required for the present method is significantly lower than that of algebraic methods. Since the complexity of the LU method is $O(n^3)$, if the DSI of the model increases, then the time difference dramatically rises.

In the present method, numbering the nodes of a finite element model is less important and only a suitable ordering of the members of the natural associate graph is required to reduce the bandwidth of the flexibility matrices.

[DOI: 10.22068/ijoce.2024.14.1.578]

ACKNOWLEDGMENT

The Corresponding author is grateful to the Islamic Azad University for the support.

REFERENCES

1. Argyris JH, Kelsey S. *Energy theorems and structural analysis*, Vol. 60, Butterworths, London, 1960.
2. Henderson JDC. Topological Aspects of Structural Linear Analysis: Improving the Conditioning of the Equations of Compatibility of a Multi-Member Skeletal Structure by Use of the Knowledge of Topology, *Aircr Eng Aerosp Technol*, 1960; **32**(5): 137-41.
3. Maunder EA. *Topological and linear analysis of skeletal structures*, 1971.
4. Henderson JDC, Maunder EA. A problem in applied topology: on the selection of cycles for the flexibility analysis of skeletal structures, *IMA J Appl Math*, 1969; **5**(2): 254-69.
5. Kaveh A. Improved cycle bases for the flexibility analysis of structures, *Comput Methods Appl Mech Eng*, 1976; **9**(3): 267-72.

6. Kaveh A. An efficient flexibility analysis of structures, *Comput struct*, 1986; **22**(6):973-
7. Kaveh A. A combinatorial optimization problem; Optimal generalized cycle bases, *Comput Methods Appl Mech Eng*, 1979; **20**(1): 39-51.
8. Cassell AC. An alternative method for finite element analysis: a combinatorial approach to the flexibility method for structural continua and to analogous methods in field analysis, *Proceedings of the Royal Society of London. A. Mathematical and Physical Sciences*, 1976; 352(1668): 73-89.
9. Denke PH. *A general digital computer analysis of statically indeterminate structures*, 1962. (No. NASA-TN-D-1666).
10. Robinson J. *Integrated theory of finite element methods*, 1973.
11. Topcu A. *A contribution to the systematic analysis of finite element structures using the force method*, Doctoral dissert, Essen Univer, 1979; 444.
12. Kaneko I, Lawo M, Thierauf G. On computational procedures for the force method, *Int J Numer Methods Eng*, 1982; **18**(10): 1469-95.
13. Soyer E, Topçu A. Sparse self-stress matrices for the finite element force method, *Int J Numer Methods Eng*, 2001; **50**(9): 2175-94.
14. Gilbert JR, Heath MT. Computing a sparse basis for the null space, *SIAM J Discret Math*, 1987; **8**(3): 446-59.
15. Coleman TF, Pothen A. The null space problem I. Complexity, *SIAM J Discret Math*, 1986; **7**(4): 527-37.
16. Coleman TF, Pothen A. The null space problem II. Algorithms, *SIAM J Discret Math*, 1987; **8**(4): 544-63.
17. Pothen A. Sparse null basis computations in structural optimization, *Numer Math*, 1989; **55**(5): 501-19.
18. Heath MT, Plemmons RJ, Ward RC. Sparse orthogonal schemes for structural optimization using the force method, *SIAM J Discret Math*, 1984; **5**(3): 514-32.
19. Patnaik S. An integrated force method for discrete analysis, *Int J Numer Methods Eng*, 1973; **6**(2): 237-51.
20. Patnaik SN, Berke L, Gallagher RH. Integrated force method versus displacement method for finite element analysis, *Comput Struct*, 1991; **38**(4): 377-407.
21. Kaveh A, Rahami H. Analysis, design and optimization of structures using force method and genetic algorithm, *Int J Numer Methods Eng*, 2006; **65**(10): 1570-84.
22. Kaveh A, Massoudi MS. Efficient finite element analysis using graph-theoretical force method tetrahedron elements, *Int J Numer Methods Eng*, 2014;**12**(2): 249-69.
23. Kaveh A, Massoudi MS, Massoudi MJ. Efficient finite element analysis using graph-theoretical force method; rectangular plane stress and plane strain serendipity family elements, *Period Polytech Civ Eng*, 2014; **58**(1): 3-22.
24. Kaveh A, Massoudi MS. Efficient finite element analysis using graph-theoretical force method; rectangular plane stress and plane strain Lagrange family elements, *Appl Math Comput*, 2015; **266**: 72-94.
25. Haji Ebrahim Araghi F, Massoudi MS, Kaveh A. Efficient Graph-Theoretical Force Method: Wedge-Shaped Finite Element, *Iran J Sci Tech, T Civ Eng*, 2021; **45**: 1121-38.
26. Kaveh A, Nasab EN. A new four-node quadrilateral plate bending element for highly sparse and banded flexibility matrices, *Acta Mech*, 2010; **209**: 295-309.

[DOI: 10.22068/ijoce.2024.14.1.578]

27. Kaveh A. Graphs and structures, *Comput Struct*, 1991; 40: 893–901.
28. Kaveh A. *Structural mechanics: graph and matrix methods*, 1992.
29. Przemieniecki JS. *Theory of matrix structural analysis*, Courier Corporation, 1985.
30. Kaveh A, Koohestani K, Taghizadeh N. Force method for finite element models with indeterminate support conditions, *Commun numer methods eng*, 2007; **8**: 389-403.
31. Kaveh A, Fazli H. Analysis of frames by substructuring technique based on using algebraic and graph methods, *Commun numer methods eng*, 2008; **24**(10): 867-74.
32. Kaveh A. *Optimal analysis of structures by concepts of symmetry and regularity*, New York, Springer, 2013.

APPENDIX A. NOTATIONS

Index	Description
FEM	finite element model
S	nodal forces
F	elemental Forces
SES	self-equilibrating system
A	equilibrium matrix
B1	self-stress matrix
Fm	unassembled flexibility matrix
G	flexibility matrix
N	number of nodes of FEM
M	number of elements of FEM
IG	interface graph
NAG	natural associate graph
NIN	negative incidence number
Type I self equilibrating system	self-equilibrium system which is constructed on a 2-multiple member
Type II self equilibrating system	self-equilibrium system which is extracted from two adjacent elements of FEM
Type III self equilibrating system	self-equilibrium system which is extracted from cycle of the NAG
DSI	degree of statical indeterminacy
M'	number of members of the associate graph of the model

[DOI: 10.22068/ijoce.2024.14.1.578]